the jet, and they become progressively less dense away from the axis of the jet. As a result, it is frequently difficult to obtain a clear definition of the boundary of the fragment cone. It is also not known what particle sizes were measured in the experiments of Ref. 7.

Burst Distances

We have taken measurements from the DFVLR data described in the previous section to estimate the burst distance of several streams at different temperatures. Some of these results have been plotted in the form of ℓn (burst distance) as a function of temperature as shown in Fig. 2. Our predictions agree with the slope of the data, but the calculated distances are shorter by a constant factor. We have plotted the natural logarithm of the predicted burst distance and have included the constant factor that best fits the data. The constant factor included in the predictions may possibly be explained by hypothesizing some effective nucleation distance that is not accounted for in our analysis (and seems to be much longer than the growth distance) in which the bubbles are developing, and they begin to grow sometime later downstream. With the inclusion of the constant factor, there is generally good agreement of prediction with experiment. It can be seen that although there is significant scatter in the data available, the burst distance decreases with increasing temperature and with decreasing velocity.

Figure 3 further illustrates the dependence of the burst distance on the stream's speed for a fixed initial temperature. The closed circles are true data points, the open circle is an interpolated point obtained from Fig. 2, the cross is the data point obtained from video-recorded data from the STS mission 61-B, and the curve is the prediction including the constant multiplier. Again, the slope of the curve is nearly identical to prediction, and it is clear that increasing the stream speed moves the burst point further downstream.

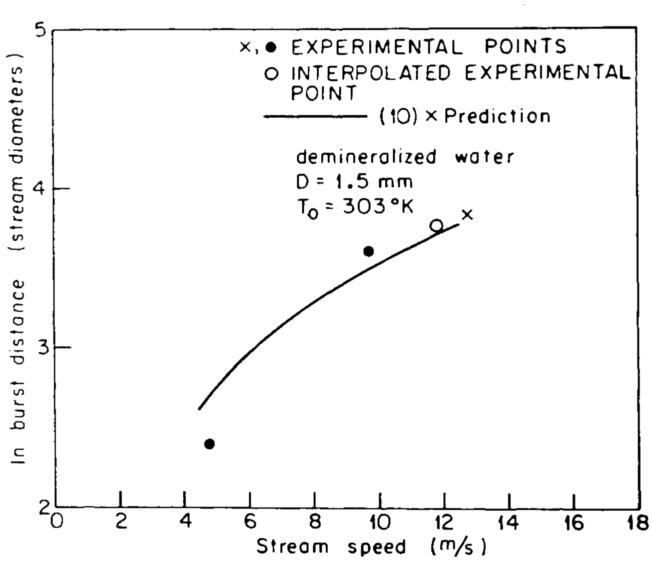

Fig. 3 Comparison of calculated to observed burst distance as a function of stream velocity for a 1.5 mm stream and an initial temperature of 303K. • Experimental data from DFVLR, o interpolated data from DFVLR, X Experimental data from STS mission 61-B.

Summary

The limiting trajectory of macroscopic particles from cavitating water streams has been predicted. In experiments where we were able to examine the original data, the predictions were quite successful. From these studies, it was found that a water stream may exist in bundled form in a vacuum without bursting if the initial water temperature is sufficiently low. Also, it was determined that increasing the stream speed increases the burst distance. Fragment cone angles of the bursts generally increase with increasing water temperature, as seen in both experiment and prediction. It was also found that acceleration of the particles due to the expanding vapor may affect significantly the burst angle. Experiments need to be done to measure particle size distribution as a function of position in the plumes of cavitating streams in a vacuum, and as a function of stream temperature in order to accurately predict the acceleration of the burst particles, thus having the ability to accurately predict the cone angle. Although some recent results of this nature[8,9] are now available for water, they are for streams that have cavitated close to the nozzle throat. The cavitation locations of Refs. 8 and 9 are in substantial disagreement (greater than one order of magnitude) with the burst distances observed in the experiments reported in Ref. 1.

Acknowledgment

This work was, in part, supported by the U.S. Air Force Rocket Propulsion Laboratory under Contract F04611-84-K-0026.

References

[1]Fuchs, H. and Legge, H., "Flow of Water Jet into Vacuum," *Acta Astronautica,* Vol. 6, 1979, pp. 1213–1226.

[2]Muntz, E.P. and Orme, M., "The Characteristics, Control, and Uses of Liquid Streams in Space," *AIAA Journal* (submitted for publication).

[3]Van Stralen, S. and Cole, R., *Boiling Phenomena,* edited by S. Van Stralen and R. Cole, McGraw-Hill, New York, 1979, Vol. 1, Chap. 7, p. 197.

[4]Wu, K.J., Steinberger, R.L., and Bracco, F.V., "On the Mechanism of Breakup of Highly Superheated Liquid Jets," The Combustion Institute Central States Section, Spring Meeting, Warren, MI, 1981.

[5]Knight, C.J., "Evaporation from a Cylindrical Surface into Vacuum," *Journal of Fluid Mechanics,* Vol. 75, 1976, pp. 469–486.

[6]Bednarz, J., "Astro Innovations," (private communication) Feb. 1987.

[7]Steddum, F., Maples, D., and Donovan, M., "Investigation on the Characteristics of Fluids Vented into Vacuum," NBS Space Simulation 56, 905–914, 1970.

[8]Curry B.P., Bryson, R.J., Seiber, B.L., Jones, J.H., Kiech, E.L., and Powell, H.M., "Preliminary Results of the AEDC Liquid Venting Experiment," *Proceedings of the 14th JANNAF Plume Technology Meeting,* CPI Publication 384, Vol. 2, Nov. 1983, pp. 105–116.

[9]Curry, B.P., Bryson, R.J., Seiber, B.L., and Kiech, E.L., "Additional Results from an Experiment Venting and H_2O Jet into a High Vacuum," Calspan Corporation, AEDC Division, Final Rept. AD B096121, June 1985.

Perturbation Analysis of Tapered Fins with Nonlinear Thermal Properties

Kirk D. Hagen*
UNISYS Corporation, Salt Lake City, Utah

Introduction

THE use of perturbation techniques for the analysis of heat conduction in fins with nonlinear thermal properties may be found in several recent studies. Perturbation methods are computationally efficient and are sufficiently accurate for fin design purposes. Indeed, Aziz and Na[1] have devoted an entire book to the subject of perturbation methods for heat transfer problems.

Received Nov. 7, 1986; revision received May 12, 1987.

*Principal Engineer, Advanced Engineering Analysis/Design.

Temperature dependence of thermal conductivity has been treated by Aziz and Enamul Huq[2] and Aziz and Benzies[3] using a regular perturbation series. Variations of these solutions to include internal generation and periodic base temperature have been reported by Aziz[4] and Aziz and Na,[5] respectively. The analysis of fins cooled by laminar and turbulent natural convection and heated by laminar condensation is also given in Ref. 3. The nonlinearity due to radiation from fins to surroundings has been treated by Bilenas and Jiji,[6] among others.

These studies dealt with longitudinal fins of rectangular profile. This paper consolidates previous results for the nonlinear effects of temperature-dependent thermal conductivity and heat transfer coefficient for natural convection while allowing for a profile deviation from rectangular to trapezoidal. The inclusion of this profile perturbation in the analysis should be considered in the design process to obtain the optimum fin. The solution of this problem is given here.

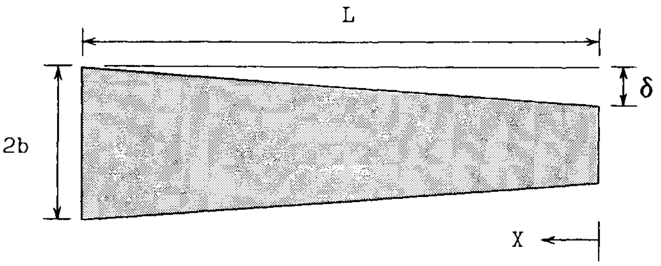

Fig. 1 Tapered fin.

Analysis

Consider a thin, symmetric longitudinal fin of length L and base thickness $2b$, as shown in Fig. 1. The cross-sectional area of the fin for a unit depth is given by

$$A(x) = 2[b + \delta(x/L - 1)] \tag{1}$$

The fin tip is assumed to be adiabatic, and the base is maintained at a constant temperature T_b. The surrounding fluid temperature is T_∞. The thermal conductivity of the fin varies linearly with temperature according to

$$k(T) = k_0[1 + \beta(T - T_\infty)] \tag{2}$$

where k_0 is a reference conductivity and β is the slope of $k(T)$. The heat transfer coefficient for fins cooled by natural convection can be expressed in the form[7]

$$h(T) = C(T - T_\infty)^n \tag{3}$$

where C is a constant and n is 0.25 and 0.33 for laminar and turbulent conditions, respectively. It should be noted that h can also be a function of the coordinate x.[8]

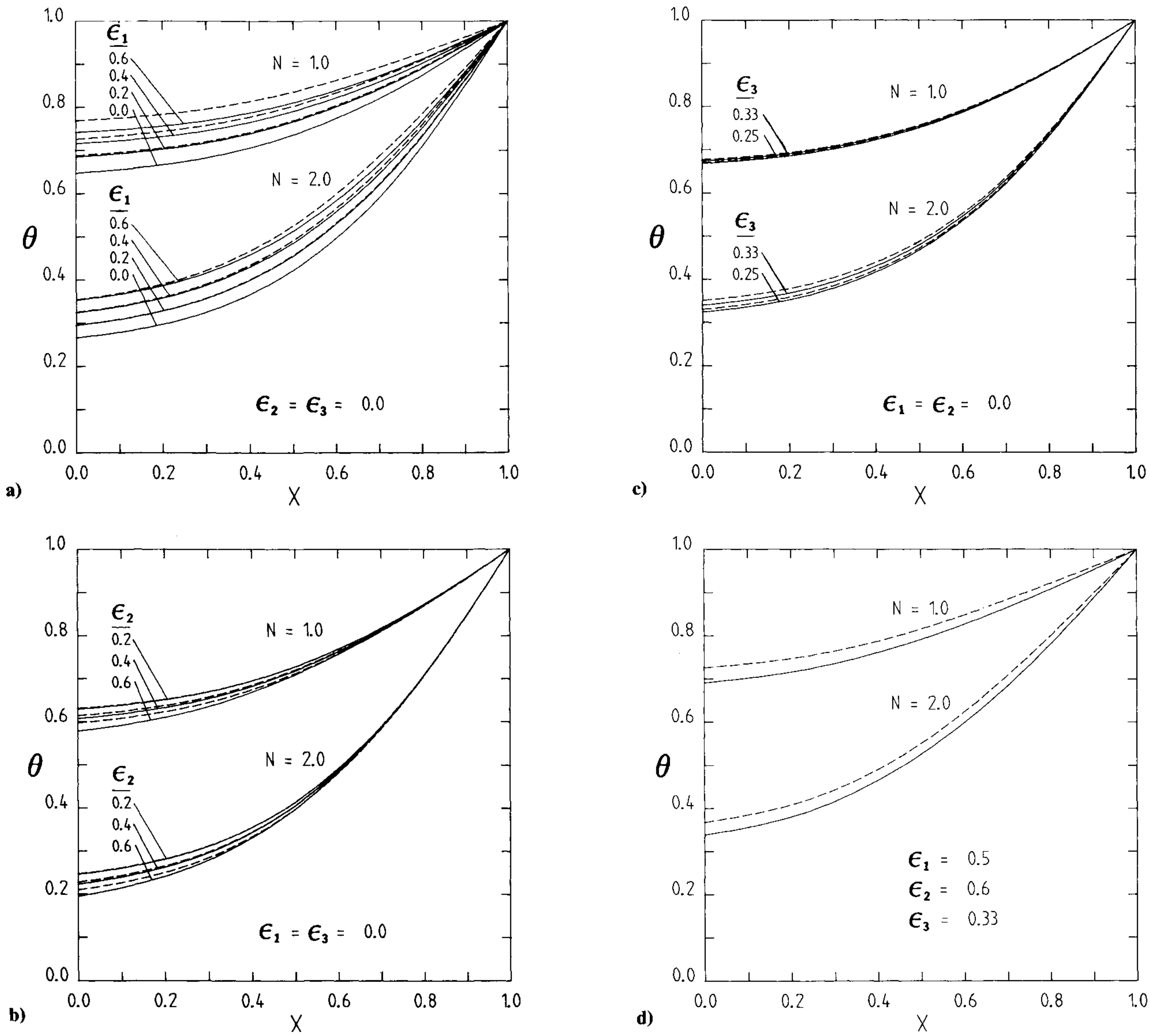

Fig. 2 Comparisons of perturbation and numerical solutions for a tapered fin:---, perturbation solution;—, numerical solutions.

We assume a first-order perturbation expansion for the dimensionless temperature $\theta=(T-T_\infty)/(T_b-T_\infty)$ as

$$\theta=\theta_0+\epsilon_1\theta_1+\epsilon_2\theta_2+\epsilon_3\theta_3 \tag{4}$$

where ϵ_1, ϵ_2, and ϵ_3 represent the small parameters associated with nonlinear thermal conductivity, fin profile deviation, and nonlinear heat transfer coefficient, respectively. By defining a dimensionless coordinate $X=x/L$ and making use of Eqs. (1-3), the governing equations for heat transfer in the fin become

$$\frac{\mathrm{d}}{\mathrm{d}X}\left\{(1+\epsilon_1\theta)\left[1+\epsilon_2(X-1)\right]\frac{\mathrm{d}\theta}{\mathrm{d}X}\right\}-N^2\theta\epsilon_3+1=0$$

$$\theta(1)=1; \qquad \frac{\mathrm{d}\theta(0)}{\mathrm{d}X}=0 \tag{5}$$

where

$$\epsilon_1=\beta\theta_b; \quad \epsilon_2=\frac{\delta}{b}; \quad \epsilon_3=n;$$

$$N^2=\frac{C\theta_b^{\epsilon_3}L^2}{k_0 b}; \quad \theta_b=T_b-T_\infty \tag{6}$$

Upon substitution of Eq. (4) into Eq. (5) and equating like orders of ϵ, the temperature distribution corresponding to each perturbation parameter can be obtained.

The governing equations for the zero-order problem are

$$\frac{\mathrm{d}^2\theta_0}{\mathrm{d}X^2}-N^2\theta_0=0; \qquad \theta_0(1)=1; \qquad \frac{\mathrm{d}\theta_0(0)}{\mathrm{d}X}=0 \tag{7}$$

and the solution is

$$\theta_0=\operatorname{sech}N\cosh NX \tag{8}$$

The governing equations and solution for the problem of order ϵ_1 are

$$\frac{\mathrm{d}^2\theta_1}{\mathrm{d}X^2}-N^2\theta_1=-\frac{\mathrm{d}}{\mathrm{d}X}\frac{(\theta_0\mathrm{d}\theta_0)}{\mathrm{d}X};$$

$$\theta_1(1)=0; \qquad \frac{\mathrm{d}\theta_1(0)}{\mathrm{d}X}=0 \tag{9}$$

and

$$\theta_1=\tfrac{1}{3}\operatorname{sech}^2N(\operatorname{sech}N\cosh 2N\cosh Nx-\cosh 2Nx) \tag{10}$$

For the remaining orders, the boundary conditions are identical in form to those of Eq. (9). For order ϵ_2, the governing equation and solution are

$$\frac{\mathrm{d}^2\theta_2}{\mathrm{d}X^2}-N^2\theta_2=-\frac{\mathrm{d}}{\mathrm{d}X}\left[(X-1)\frac{\mathrm{d}\theta_0}{\mathrm{d}X}\right] \tag{11}$$

and

$$\begin{aligned}\theta_2=&(\tfrac{1}{4}N)\operatorname{sech}^2N\{(\cosh N-\sinh N)\cosh NX\\&+N\cosh N(1-N\tanh N)\cosh N^x\\&-(\cosh NX-\sinh NX)\cosh N\\&-NX\cosh N[N(X-2)\sinh NX+\cosh NX]\}\end{aligned} \tag{12}$$

It is to be noted that, unlike the problems of order ϵ_1 and ϵ_3, the problem of order ϵ_2 is a linear perturbation, which can be seen in Eq. (5). The method for linear perturbation series discussed by Bellman[9] applies in this case.

Finally, the governing equation for order ϵ_3 is

$$\frac{\mathrm{d}^2\theta_3}{\mathrm{d}X^2}-N^2\theta_3=N^2\theta_0\,\ln\theta_0 \tag{13}$$

Aziz and Benzies[3] approximated the nonhomogeneous term in Eq. (13) using an eighth-order Maclaurin series. As shown by Arunachalam and Seeniraj,[10] an exact solution is possible using a variation of parameters. This solution, however, is somewhat longer and involves two infinite series, so the series approximation is chosen here. The solution is

$$\begin{aligned}\theta_3=&C_1\cosh NX+C_2X\sinh NX-C_3\left[84+42(NX)^2\right.\\&\left.+41/12\,(NX)^4+37/360\,(NX)^6+1/560\,(NX)^8\right]\end{aligned} \tag{14}$$

where

$$\begin{aligned}C_1=&\tfrac{1}{2}\operatorname{sech}^2N(84+42N^2+41/12N^4+37/360N^6\\&+1/560N^8)-\tfrac{1}{2}N\tanh N\operatorname{sech}N\ln(\operatorname{sech}N)\\C_2=&\tfrac{1}{2}N\operatorname{sech}N\ln(\operatorname{aech}N)\\C_3=&\tfrac{1}{2}\operatorname{sech}N\end{aligned} \tag{15}$$

Discussion and Results

Equation (5) was solved numerically using a fourth-order Runge-Kutta method to check the accuracy of the perturbation solution. Figure 2a compares the numerical and perturbation temperature profiles for $N=1.0$ and 2.0 and for various values of ϵ_1, while holding ϵ_2 and ϵ_3 to zero. The agreement is excellent particularly for small values of ϵ_1 and for $N=2.0$ where the sensitivity to thermal conductivity dependence on the temperature is relatively low. The maximum error shown is 3.6% and occurs at the fin tip for $\epsilon_1=0.6$ and $N=1.0$. Only positive values of ϵ_1 are given here; negative values yield the same accuracy.

Figure 2b compares the numerical and perturbation temperatures for various values of the fin profile parameter ϵ_2 while holding ϵ_1 and ϵ_3 to zero. For the majority of commercially available fin stock, the magnitude of ϵ_2 ranges from 0 to 0.6. Of course, negative values of ϵ_2 have no physical meaning. As illustrated, the departure from the numerical solution for this range of ϵ_2 is very small. The maximum difference shown is about 3.3%. Snider and Kraus[11] reported similar accuracy in corrections of up to 10% in the thermal transmission matrix for a trapezoidal fin. It should be noted that an exact solution for the problem of order ϵ_2 only has been carried out

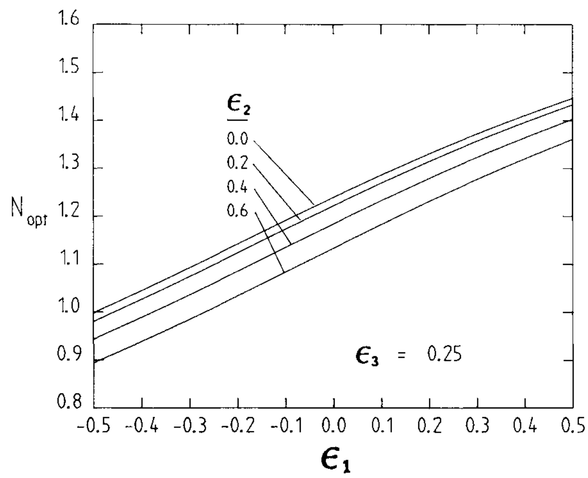

Fig. 3 Optimum N for laminar natural convection.

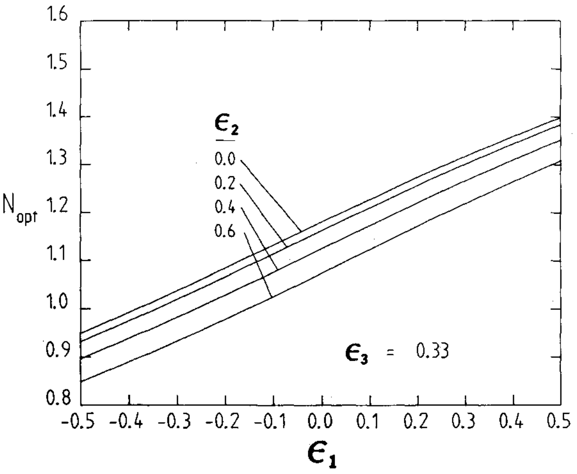

Fig. 4 Optimum N for turbulent natural convection.

by Kraus,[12,13] in terms of modified Bessel function and is essentially identical to the numerical solution given here.

Figure 2c compares the numerical and perturbation results for $\epsilon_3 = 0.25$ and 0.33 while holding ϵ_1 and ϵ_2 to zero. The maximum difference shown for this case is 2.0%.

Finally, Fig. 2d compares the numerical and perturbation solutions for $\epsilon_1 = 0.5$, $\epsilon_2 = 0.6$, and $\epsilon_3 = 0.33$. These values represent a worst case in which the perturbation parameters are maximum in the practical application range. The maximum error in this case is 7.3%.

The fin efficiency, η, is readily calculated by dividing the heat transfer q through the base by the ideal heat transfer rate. The result is

$$\begin{aligned}\eta = 1/N^2 \{ & (1+\epsilon_1)N \tanh N + (\epsilon_1/3)N \tanh N(\tanh^2 N - 3) \\ & + (\epsilon_2/8)\,\mathrm{sech}^2 N(2N^2 + 1 - \cosh 2N - \sinh 2N) \\ & + \epsilon_3 [C_1 N \sinh N + C_2(\sinh N + N \cosh N) \\ & - C_3(84N^2 + 41/3\, N^4 + 37/60\, N^6 + 1/70\, N^8)] \} \end{aligned} \tag{16}$$

The fin can be optimized with respect to volume by finding the values of b and δ that yield the maximum heat transfer for a given set of the perturbation parameters. Upon performing the derivatives $\mathrm{d}q/\mathrm{d}b + \mathrm{d}q/\mathrm{d}\delta = 0$ and solving for N, the optimum dimensions can be calculated. Given in Figs. 3 and 4 are the optimum values of N as a function of ϵ_1 and ϵ_2 for laminar and turbulent conditions, respectively. These curves may be compared with the result given by Krane,[14] in which fin taper and a temperature-dependent heat transfer coefficient were not considered. When $\epsilon_2 = \epsilon_3 = 0$, Krane's curve is duplicated. Nonzero values of ϵ_2 and ϵ_3 shift N_{opt} downward from the curve in Ref. 14.

Conclusion

A first-order, three-parameter perturbation expansion has been shown to predict accurately the temperature distribution in longitudinal tapered fins with temperature-dependent thermal conductivity and heat transfer coefficient. The solution was carried out to second order, but the accuracy was not appreciably improved over the result given by the first-order expansion. Hence, the first-order solution is sufficient for fin design. Fin efficiency and optimum dimensions have been given as a function of the perturbation parameters. These results should prove to be useful in the design of tapered fins.

References

[1]Aziz, A. and Na, T.Y., *Perturbation Methods in Heat Transfer,* Hemisphere, Washington, DC, 1984, pp. 14-15, 44-46.

[2]Aziz, A. and Enamul Huq, S.M., "Perturbation Solution for Convecting Fin with Variable Thermal Conductivity," *ASME Journal of Heat Transfer,* May 1975, pp. 300-301.

[3]Aziz, A. and Benzies, J.Y., "Application of Perturbation Techniques to Heat-Transfer Problems with Variable Thermal Properties," *International Journal of Heat and Mass Transfer,* Vol. 19, 1976, pp. 271-276.

[4]Aziz, A., "Perturbation Solution for Convective Fin with Internal Heat Generation and Temperature Dependent Thermal Conductivity," *International Journal of Heat and Mass Transfer,* Vol. 20, 1977, pp. 1253-1255.

[5]Aziz, A. and Na, T.Y., "Periodic Heat Transfer in Fins with Variable Thermal Parameters," *International Journal of Heat and Mass Transfer,* Vol. 24, 1981, pp. 1397-1404.

[6]Bilenas, J.A. and Jij, L.M., "A Perturbation Solution for Fins with Conduction, Convection, and Radiation Interaction," *AIAA Journal,* Vol. 8, 1970, pp. 168-169.

[7]Holman, J.P., *Heat Transfer,* 4th ed., McGraw-Hill, New York, 1976, p. 253.

[8]Stachiewicz, J.W., "Effect of Variation of Local Film Coefficient on Fin Performance," *ASME Journal of Heat Transfer,* Vol. 91, 1969, pp. 21-26.

[9]Bellman, R., *Perturbation Techniques in Mathematics, Physics, and Engineering,* Holt, Rinehart and Winston, New York, 1964, pp. 15-17.

[10]Arunachalam, M. and Seeniraj, V., Comments on "Application of Perturbation Techniques to Heat Transfer Problems with Variable Thermal Properties," *International Journal of Heat and Mass Transfer,* Vol. 20, 1977, pp. 803-804.

[11]Snider, A.D. and Kraus, A.D., "Recent Developments in the Analysis and Design of Extended Surface," *ASME Journal of Heat Transfer,* Vol. 105, May 1983, pp. 302-306.

[12]Kraus, A.D., *Extended Surfaces,* Spartan, Baltimore, MD, 1964, pp. 52-55, 76-78.

[13]Kraus, A.D., *Analysis and Evaluation of Extended Surface Thermal Systems,* Hemisphere, Washington, D.C., 1982, pp. 100-104.

[14]Krane, R.J., "Discussion of Perturbation Solution for Convecting Fin with Variable Thermal Conductivity," *ASME Journal of Heat Transfer,* Nov. 1976, pp. 685-686.

Correlation of the Gap Conductance Integral for Conforming Rough Surfaces

K. J. Negus* and M. M. Yovanovich†
University of Waterloo, Waterloo, Ontario, Canada

Introduction

STEADY-STATE heat transfer across the interface of two contracting solid bodies is usually accompanied by a measurable temperature drop due to the thermal resistance to heat flow in the interface region. If the temperature drop ΔT_c at the interface is obtained by extrapolation from regions "far" from the interface and Q/A_a is the steady-state heat flux based on the apparent contact area, then the joint conductance or contact coefficient of heat transfer is defined as

$$h_j = (Q/A_a)/\Delta T_c \tag{1}$$

Considerable research has been undertaken in recent years to develop models to predict joint conductance and to experimentally verify these models as discussed in detail by

Received Dec. 11, 1986; revision received May 1, 1987.

*Graduate Research Assistant, Microelectronics Heat Transfer Laboratory, Department of Mechanical Engineering. Student Member AIAA.

†Professor, Microelectronics Heat Transfer Laboratory, Department of Mechanical Engineering. Associate Fellow AIAA.